Understanding the Photophysical Properties of Chiral Dinuclear Re(I) Complexes and the Role of Re(I) in Their Complexes

Chunyu Liu,[a] Yanling Si,[b] Shaoqing Shi,[a] Guochun Yang[a],* and Xiumei Pan[a],*

a. Institute of Functional Material Chemistry, Faculty of Chemistry, Northeast Normal University, Changchun
    130024 Jilin, China.
    E-mail:yanggc468@nenu.edu.cn
b. College of Resource and Environmental Science, Jilin Agricultural University, Changchun, 130118 Jilin, China

Contents

and the assignments for complexes **3-9** at TDB3LYP/ BSII level.   **S18**

16. Calculated UV−Vis (left) and CD (right) spectra in the solution phase for complexes **3**, **5** and **8.**   **S19**

17. Molecular orbital isosurfaces involved in the main electron transitions of complexes **3-9**.   **S20**

18. Molecular orbitals involved into the main CD transition of complexes ligand **1**, complexes **2**-**9**.   **S23**
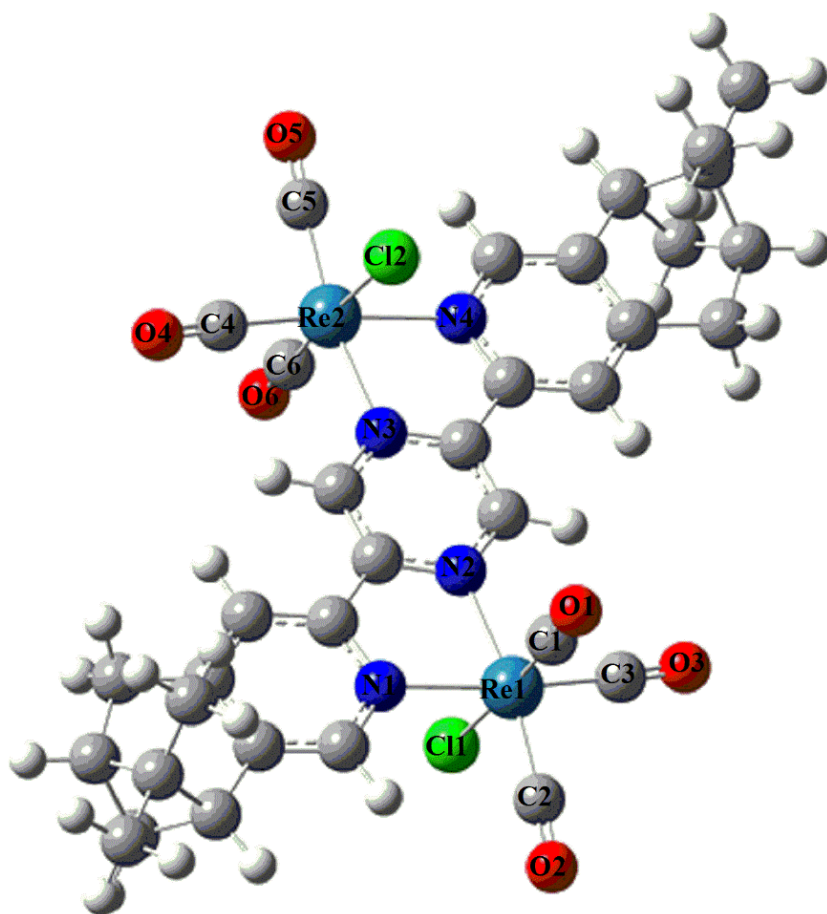
Fig S1. Optimized molecular structure and atomic label of complex **2**.

Table S1. The main concerned bond lengths and bond angles for complex **2** between experiment and calculation.

experimental					
Re(1)-N(1)	2.168	Re(1)-N(2)	2.145	Re(2)-N(3)	2.150
Re(2)-N(4)	2.147	Re(1)-C(1)	2.236	Re(1)-C(2)	1.93
Re(1)-C(3)	1.91	Re(2)-C(4)	1.87	Re(2)-C(5)	1.83
Re(2)-C(6)	1.93	Re(1)-Cl(1)	2.402	Re(2)-Cl(2)	2.420
N(2)-Re(1)-N(1)	74.9	N(4)-Re(2)-N(3)	74.5	C(2)-Re(1)-N(1)	99.7
C(1)-Re(1)-N(2)	83.8	N(3)-Re(2)-C(4)	99.9	N(4)-Re(2)-C(6)	93.2
theoretical					
Re(1)-N(1)	2.207	Re(1)-N(2)	2.194	Re(2)-N(3)	2.194
Re(2)-N(4)	2.207	Re(1)-C(1)	1.917	Re(1)-C(2)	1.93
Re(1)-C(3)	1.93	Re(2)-C(4)	1.93	Re(2)-C(5)	1.93
Re(2)-C(6)	1.92	Re(1)-Cl(1)	2.550	Re(2)-Cl(2)	2.550
N(2)-Re(1)-N(1)	74.5	N(4)-Re(2)-N(3)	74.5	C(2)-Re(1)-N(1)	97.7
C(1)-Re(1)-N(2)	93.6	N(3)-Re(2)-C(4)	97.55	N(4)-Re(2)-C(6)	93.0

Table S2. Selected calculated IR vibrational frequencies (cm^{-1}) along with the experimental data (in parentheses) of complex **2**.

vibrational frequencies	Vibrational assignment
1934(1907)	$\upsilon_{asym}(C\equiv O)$
2002(2019)	$\upsilon_{sym}(C\equiv O)$
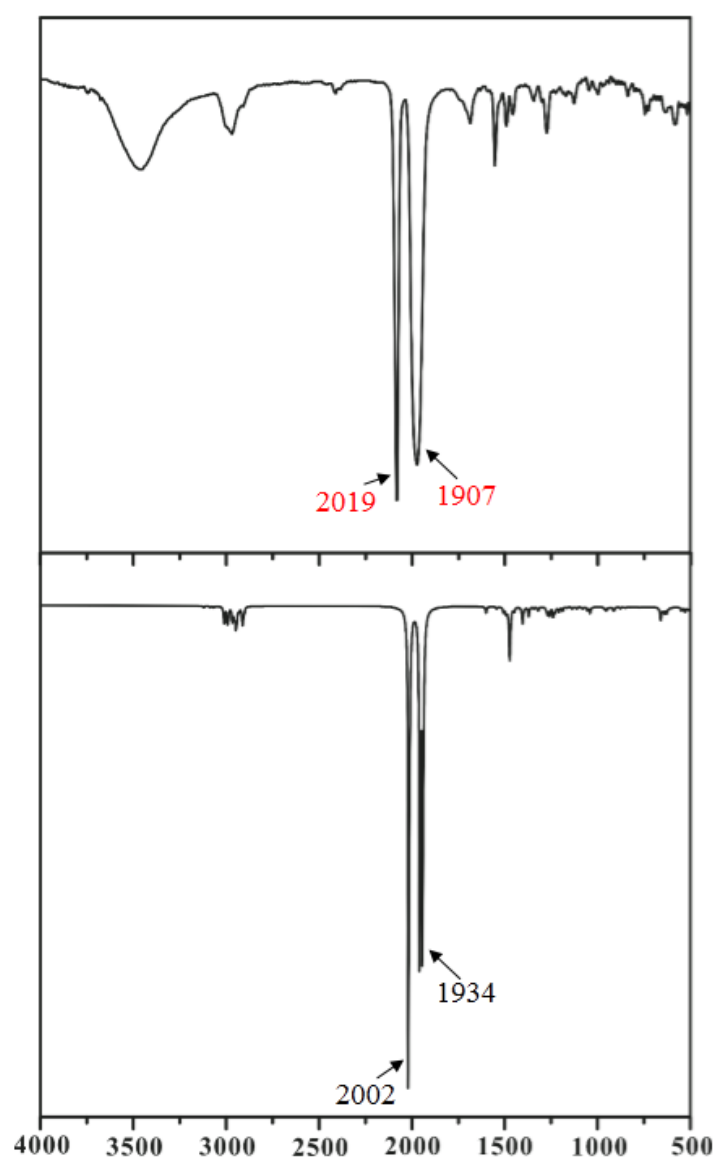
Figure S2. The calculated IR spectra of complex **2** at B3LYP/BSI level along with the experimental data (labeled as red). The experimental data can be found in ref.34.

2   **3**   **8**

Figure S3. The selected atomic labels of complexes **2**, **3** and **8**.

Table S3. The binding energies (ΔE) (kcal/mol) for complexes **2**, **3** and **8**.

Complex	ΔE
2	-47
3	-48
8	-44

Table S4. Second order perturbation interactions that contribute mainly to the ground state stabilization for complexes **2**, **3** and **8** from NBO analysis performed at the B3LYP/BSI level.

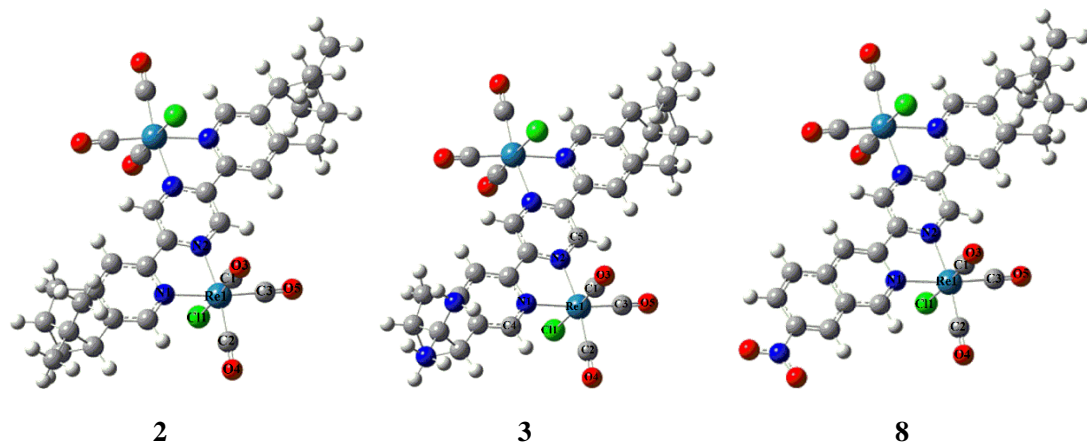| Complex	Donor (i)	Acceptor(j)	$E(2)$(kcalmol^{-1})	E(j)-E(i) a.u	F(i, j) a.u
2	n Re(1)	σ* Re(1) – Cl(1)	15.44	0.39	0.077
	n Re(1)	σ* Re(1) – N(1)	110.03	0.12	0.126
	n Re(1)	σ* Re(1) – N(2)	28.33	0.25	0.082
	n Re(1)	σ* Re(1) – C(1)	14.32	0.55	0.089
	n Re(1)	σ* Re(1) – C(2)	54.26	0.34	0.152
	n Re(1)	σ* Re(1) – C(3)	60.08	0.33	0.160
3	n Re(1)	σ* Re(1) – Cl(1)	4.80	0.39	0.073
	n Re(1)	σ* N(1) – C(4)	1.09	0.60	0.027
	n Re(1)	σ* N(2) – C(5)	1.23	0.60	0.029
	n Re(1)	σ* Re(1) – C(1)	29.12	0.48	0.121
	n Re(1)	σ* Re(1) – C(2)	64.25	0.43	0.165
	n Re(1)	σ* Re(1) – C(3)	67.80	0.43	0.169
8	n Re(1)	σ* Re(1) – Cl(1)	17.42	0.39	0.081
	n Re(1)	σ* Re(1) – N(1)	109.45	0.12	0.124
	n Re(1)	σ* Re(1) – N(2)	100.61	0.12	0.120
	n Re(1)	σ* Re(1) – C(1)	15.68	0.54	0.093
	n Re(1)	σ* Re(1) – C(2)	56.67	0.33	0.155
	n Re(1)	σ* Re(1) – C(3)	59.53	0.34	0.159

Table S5. Frontier molecular orbital compositions (%) in the ground state for complex **2** at the B3LYP/BSII (BSIII for metal Re) level.

Orbital	Energy (eV)	Contribution (%)				Main bond type
		Re	CO	Cl	L_R	
L+4	-1.45	2.53	2.69	0.04	94.74	$\pi^*(L_R)$
L+3	-1.75	0.01	2.82	0.09	97.08	$\pi^*(L_R)$
L+2	-2.03	3.64	7.12	0.80	88.43	$\pi^*(L_R)$
L+1	-2.70	-0.56	1.68	0.20	98.68	$\pi^*(L_R)$
L	-3.62	4.11	4.93	1.00	89.96	$\pi^*(L_R)$
HOMO-LUMO Energy gap(2.86 eV)						
H	-6.48	47.62	24.27	24.03	4.09	$d(Re)+ \pi (CO)+ p(Cl)$
H-1	-6.51	47.34	23.16	25.33	4.17	$d(Re)+ \pi (CO)+ p(Cl)$
H-2	-6.54	48.20	21.77	25.29	4.73	$d(Re)+ \pi (CO)+ p(Cl)$
H-3	-6.68	41.18	18.12	34.28	6.42	$d(Re)+ \pi (CO)+ p(Cl)$
H-4	-7.05	68.47	30.45	0.62	0.46	$d(Re)+ \pi (CO)$
H-5	-7.06	68.19	30.74	0.46	0.62	$d(Re)+ \pi (CO)$
H-6	-7.14	0.26	0.08	2.95	96.71	$\pi(L_R)$
H-7	-7.63	3.00	1.69	30.81	64.49	$p(Cl) +\pi(L_R)$
H-8	-7.74	9.03	3.80	56.57	30.60	$p(Cl) +\pi(L_R)$
H-9	-7.84	14.89	6.67	70.44	8.00	$d(Re)+p(Cl)$

Table S6. Frontier molecular orbital compositions (%) in the ground state for complex **3** at the B3LYP/BSII level.

Orbital	Energy (eV)	Contribution (%)				Main bond type
		Re	CO	Cl	L_R-NH_2NH_2	
L+4	-1.41	2.52	2.82	0.03	94.62	$\pi^*(L_R\text{-}NH_2NH_2)$
L+3	-1.70	0.26	3.07	0.10	96.57	$\pi^*(L_R\text{-}NH_2NH_2)$
L+2	-1.99	3.78	7.40	0.80	88.02	$\pi^*(L_R\text{-}NH_2NH_2)$
L+1	-2.68	-0.57	1.68	0.19	98.70	$\pi^*(L_R\text{-}NH_2NH_2)$
L	-3.60	4.12	4.94	0.99	89.96	$\pi^*(L_R\text{-}NH_2NH_2)$
HOMO-LUMO Energy gap(2.86 eV)						
H	-6.46	43.75	22.18	21.41	12.66	$d(Re)+\pi(CO)+p(Cl)$
H-1	-6.49	46.45	22.82	24.24	6.49	$d(Re)+\pi(CO)+p(Cl)$
H-2	-6.53	46.40	21.16	24.02	8.42	$d(Re)+\pi(CO)+p(Cl)$
H-3	-6.61	6.61	3.11	5.31	84.98	$\pi(L_R\text{-}NH_2NH_2)$
H-4	-6.67	41.21	18.14	34.24	6.41	$d(Re)+p(Cl)$
H-5	-7.04	68.38	30.51	0.60	0.50	$d(Re)+\pi(CO)$
H-6	-7.05	68.22	30.73	0.45	0.60	$d(Re)+\pi(CO)$
H-7	-7.16	0.15	0.06	2.58	97.20	$\pi(L_R\text{-}NH_2NH_2)$
H-8	-7.65	4.33	2.25	37.98	55.45	$p(Cl)+\pi(L_R\text{-}NH_2NH_2)$
H-9	-7.72	8.39	3.62	55.40	32.59	$p(Cl)+\pi(L_R\text{-}NH_2NH_2)$

Table S7. Frontier molecular orbital compositions (%) in the ground state for complex **6** at the B3LYP/BSII level.

Orbital	Energy (eV)	Contribution (%)				Main bond type
		Re	CO	Cl	L_R-ph	
L+4	-1.59	0.95	1.95	0.03	97.07	$\pi^*(L_R$-ph)
L+3	-1.97	3.23	6.20	0.57	90.01	$\pi^*(L_R$-ph)
L+2	-2.42	0.71	1.76	0.00	97.53	$\pi^*(L_R$-ph)
L+1	-2.79	-0.22	1.94	0.32	97.95	$\pi^*(L_R$-ph)
L	-3.59	3.60	4.45	0.87	91.08	$\pi^*(L_R$-ph)
HOMO-LUMO Energy gap(2.90 eV)						
H	-6.49	47.67	23.86	24.37	4.10	d(Re)+ π (CO)+ p(Cl)
H-1	-6.50	46.43	22.78	24.38	6.41	d(Re)+ π (CO)+ p(Cl)
H-2	-6.54	47.32	21.58	25.00	6.11	d(Re)+ π (CO)+ p(Cl)
H-3	-6.66	39.99	17.84	32.10	10.07	d(Re)+ π (CO)+ p(Cl)
H-4	-6.96	2.60	1.10	5.86	90.44	π (L_R- ph)
H-5	-7.05	68.44	30.46	0.53	0.57	d(Re)+ π (CO)
H-6	-7.07	68.46	30.69	0.59	0.26	d(Re)+ π (CO)
H-7	-7.51	0.57	0.39	17.43	81.61	π (L_R- ph)
H-8	-7.73	7.71	3.47	51.69	37.12	p(Cl) +π (L_R- ph)
H-9	-7.82	12.16	4.77	56.24	26.82	p(Cl) +π (L_R- ph)

Table S8. Frontier molecular orbital compositions (%) in the ground state for complex **7** at the B3LYP/BSII level.

| Orbital	Energy (eV)	Contribution (%)				Main bond type
		Re	CO	Cl	L_R-NH$_2$	
L+4	-1.46	3.01	4.37	0.08	92.54	π^*(L_R-NH$_2$)
L+3	-1.87	3.01	6.43	0.55	90.01	π^*(L_R-NH$_2$)
L+2	-2.30	0.85	2.01	0.03	97.11	π^*(L_R-NH$_2$)
L+1	-2.65	-0.40	1.80	0.28	98.31	π^*(L_R-NH$_2$)
L	-3.46	3.60	4.63	0.87	90.90	π^*(L_R-NH$_2$)
HOMO-LUMO Energy gap(2.71 eV)						
H	-6.17	2.23	1.24	0.89	95.63	π(L_R-NH$_2$)
H-1	-6.45	47.77	24.04	24.26	3.94	d(Re)+ π (CO)+ p(Cl)
H-2	-6.47	46.71	23.13	24.91	5.26	d(Re)+ π (CO)+ p(Cl)
H-3	-6.51	47.73	21.84	25.12	5.31	d(Re)+ π (CO)+ p(Cl)
H-4	-6.65	39.98	17.71	33.26	9.05	d(Re)+ π (CO)+ p(Cl)
H-5	-7.01	68.54	30.49	0.60	0.36	d(Re)+ π (CO)
H-6	-7.02	68.29	30.92	0.46	0.33	d(Re)+ π (CO)
H-7	-7.32	-0.04	0.15	5.63	94.27	π(L_R-NH$_2$)
H-8	-7.53	1.50	0.88	32.55	65.08	p(Cl) +π(L_R-NH$_2$)
H-9	-7.72	8.63	3.71	53.14	34.52	p(Cl) +π(L_R-NH$_2$)
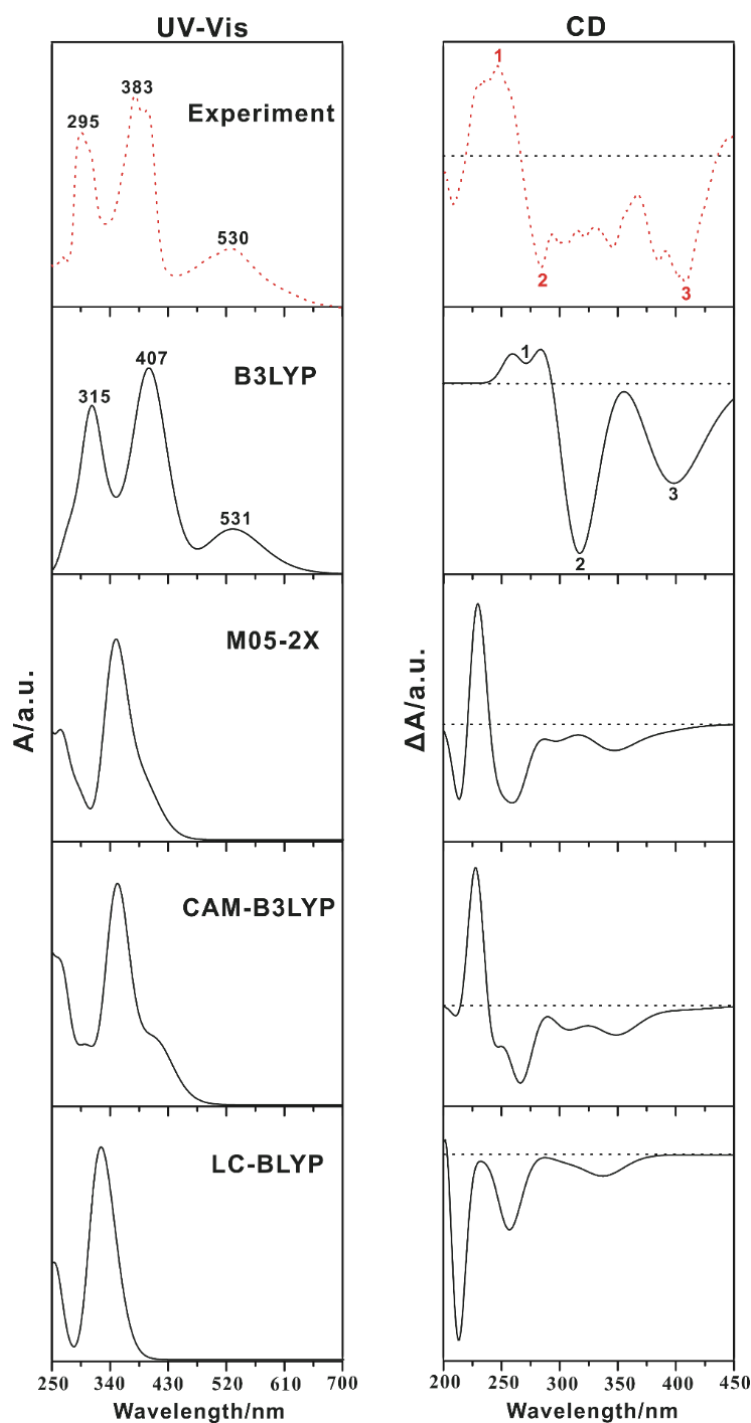
Figure S4. Calculated UV-Vis and CD spectra of complex **2** using four different DFT functionals along with the experimental spectra in solution phase. Data to prepare the experimental spectra were taken from ref.34.

It is well known that conventional TDDFT methods usually underestimate charge-transfer excitations due to semi-local exchange correlation effects. Studies have shown that range-separated functionals (e.g. LC-BLYP and CAM-B3LYP) can accurately describe electron excitation properties and calculate HOMO–LUMO gaps, and ionization/electron affinity energies. Moreover, the range-separated functionals have successfully described the optoelectronic and excitonic properties of oligoacenes.

14

Thus, we selected the both conventional and range-separated DFT functionals as follows: B3LYP, M05-2X, CAM-B3LYP, LC-BLYP to evaluate the influence of these DFT functionals on UV-Vis and CD spectra. The results show that the computed absorption wavelengths strongly depend on the used functionals. The M05-2X, CAM-B3LYP and LC-BLYP functionals could not reproduce the experimental absorption band at about 530 nm. The same blue-shifted trend was also observed in simulated CD spectra, especially for the LC-BLYP functional, the band 1 of the CD spectra is a negative Cotton effect. These observation might result from the larger energy gaps of the three functionals (CAM-B3LYP, LC-BLYP and M05-2X). However, the results computed with the B3LYP functional are much closer to the experimental results.
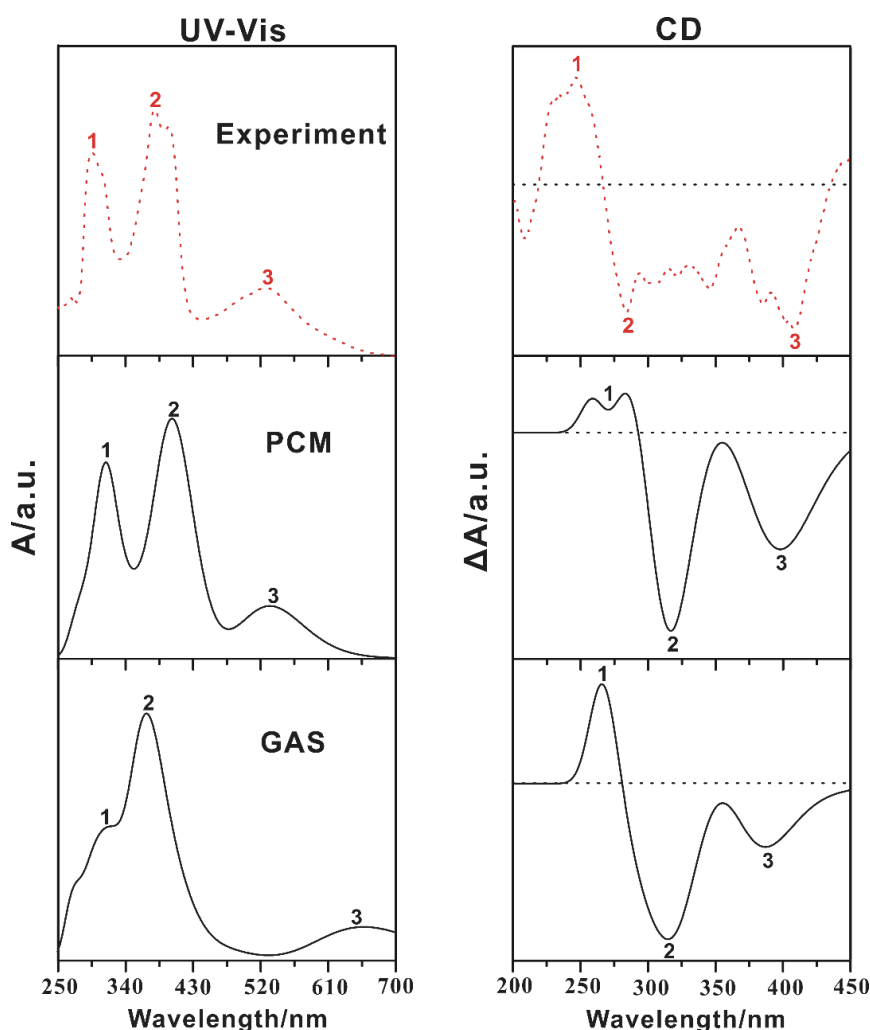

Figure S5. Calculated UV−Vis (left) and CD (right) spectra in both gas and solution phases for complex **2** at the TDB3LYP/ BSII (BSIII for metal Re) level along with experimental spectra. Data to prepare the experimental spectra were taken from ref.34.

Table S9. The calculated excitation energies, oscillator strengths and rotational strengths for complex **2** in the solution phase at the TDB3LYP/ BSII (BSIII for metal Re) level.

states	eV	λ[a]	f[b]	Rlength[c]	Rvelocity[c]
1	2.1781	569.22	0.0010	-0.0377	0.0062
2	2.1982	564.02	0.0000	0.0324	-0.1422
3	2.3366	530.63	0.1822	-0.1702	-0.0913
4	2.4730	501.36	0.0000	-0.2585	-0.2664
5	2.7161	456.48	0.0000	0.1489	0.1161
6	2.7245	455.06	0.0005	0.2612	0.2692
7	3.0428	407.47	0.4986	-2.6274	-3.0633
8	3.1090	398.79	0.1212	-4.2194	-3.7821
9	3.1208	397.28	0.0004	0.6364	0.7249
10	3.1895	388.72	0.2555	-7.9679	-5.6177
11	3.3105	374.52	0.0000	-0.1113	-0.0973
12	3.4462	359.77	0.0004	0.6628	0.5241
13	3.5036	353.87	0.0865	2.4550	2.3009
14	3.5642	347.86	0.0972	-0.4565	-0.3786
15	3.6507	339.62	0.0000	-0.2586	-0.2007
16	3.6584	338.90	0.0021	0.1490	0.2313
17	3.6903	335.97	0.0001	-0.0708	-0.0446
18	3.8033	325.99	0.0002	-3.0595	-3.0692
19	3.8476	322.24	0.0001	2.5885	2.5268
20	3.8799	319.55	0.1325	5.1682	4.4824
21	3.9252	315.87	0.0010	2.8147	2.5226
22	3.9310	315.40	0.2493	-28.9511	-26.3036
23	4.0130	308.96	0.0081	5.2493	3.8625
24	4.0257	307.98	0.2584	4.1819	3.7324
25	4.0880	303.29	0.0006	-2.4498	-2.6568
26	4.1487	298.85	0.0001	2.2214	2.2777
27	4.1521	298.61	0.0119	-3.5708	-3.5261
28	4.1951	295.54	0.0002	-4.0700	-4.1235
29	4.2022	295.05	0.0337	18.6915	18.9625
30	4.2186	293.90	0.0259	-23.9861	-25.2799
31	4.2215	293.69	0.0024	5.3776	5.8957
32	4.2273	293.29	0.0046	-9.5752	-9.9228
33	4.2380	292.56	0.0165	14.9609	15.2077
34	4.2771	289.88	0.0111	0.7766	0.6022
35	4.2898	289.02	0.0000	0.0575	-0.0586
36	4.2964	288.58	0.0022	-0.0420	-0.1839
37	4.3219	286.87	0.0002	-1.1836	-1.3155
38	4.3370	285.87	0.0003	-0.1913	-0.3266

39	4.3427	285.50	0.0003	-1.1516	-1.1168
40	4.3564	284.60	0.0063	5.5338	5.0699
41	4.3737	283.48	0.0000	-0.3406	-0.3092
42	4.3879	282.56	0.0575	7.7619	7.9637
43	4.4286	279.96	0.0010	-6.3918	-5.8940
44	4.4572	278.17	0.0058	-1.1220	-1.0756
45	4.4938	275.90	0.0513	3.3075	3.3502
46	4.4998	275.53	0.0000	-0.1652	-0.1780
47	4.5268	273.89	0.0045	-0.9497	-1.0826
48	4.5406	273.05	0.0000	0.5916	0.6352
49	4.5747	271.02	0.0003	-8.8468	-8.5337
50	4.5896	270.14	0.0448	0.4046	0.1270
51	4.6075	269.09	0.0000	3.3847	3.3173
52	4.6464	266.84	0.0001	-0.4578	-0.5859
53	4.6503	266.62	0.0002	-4.6057	-5.0510
54	4.6596	266.08	0.0008	4.6831	4.6358
55	4.6748	265.22	0.0000	3.6345	3.8033
56	4.7034	263.61	0.0047	0.1242	0.1937
57	4.7117	263.14	0.0001	0.6156	0.7680
58	4.7376	261.70	0.0000	0.0347	-0.0130
59	4.7413	261.50	0.0039	0.4716	0.3445
60	4.7920	258.73	0.0000	-0.0803	-0.0189

[a]λ in nm. [b] Oscillator Strengths. [c] R values (in 10^{-40} esu^{2}cm^2) using the velocity-gauge representation and length-gauge representation of the electric dipole operator.

Table S10. Computed energies/wavelengths (nm), oscillator strengths (*f*), major contribution and the assignments for complexes **3-9** at TDB3LYP/ BSII (BSIII for metal Re) level.

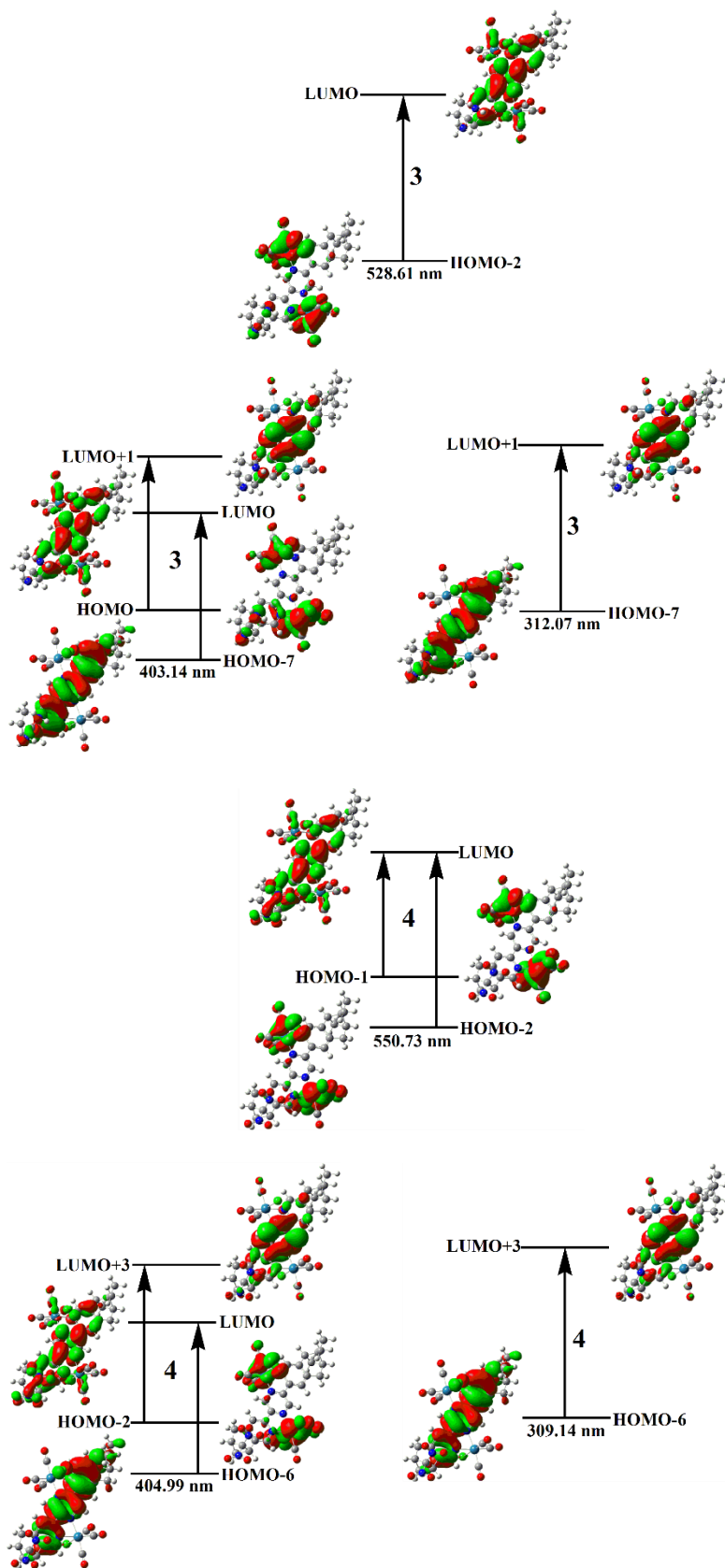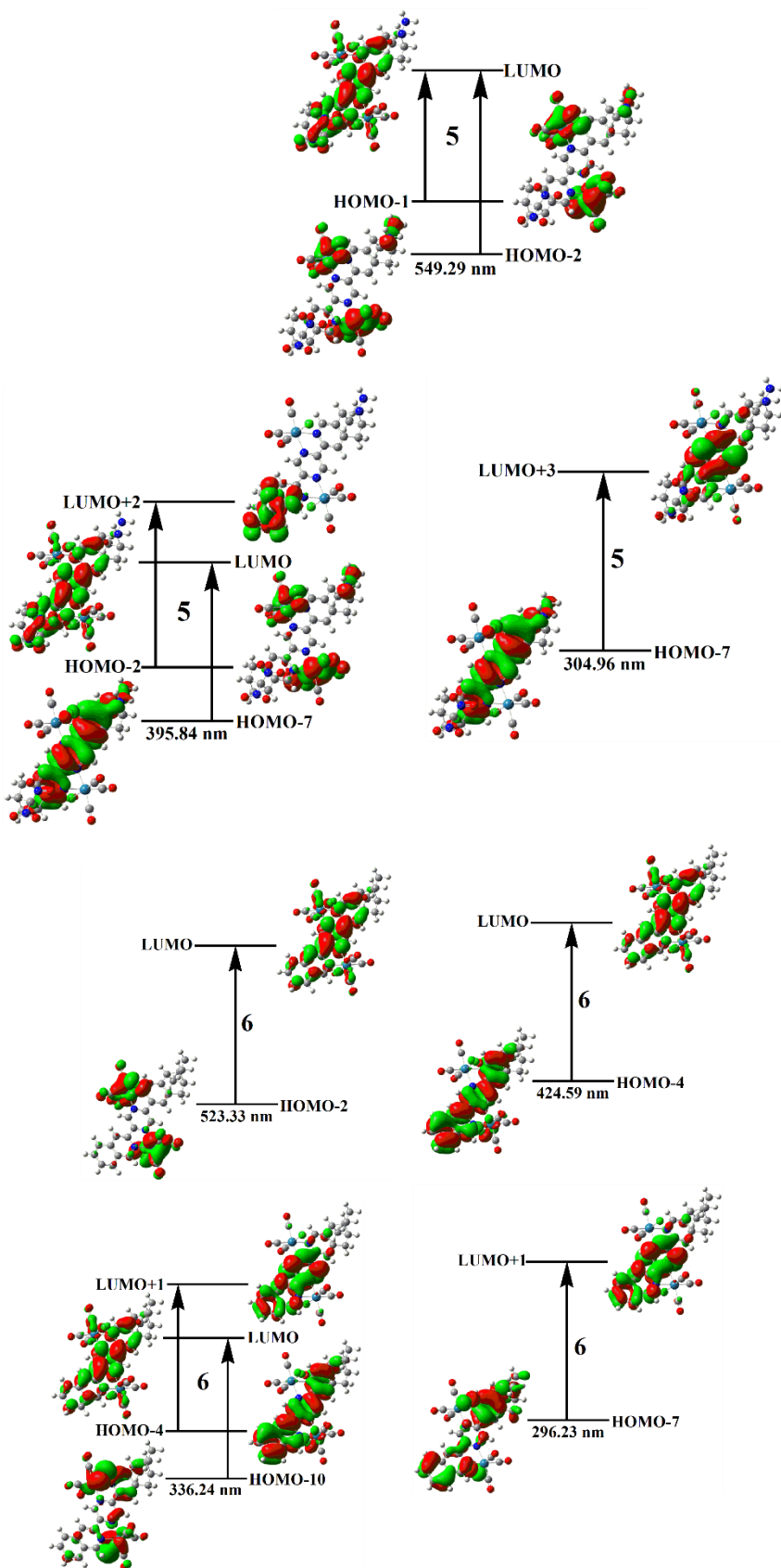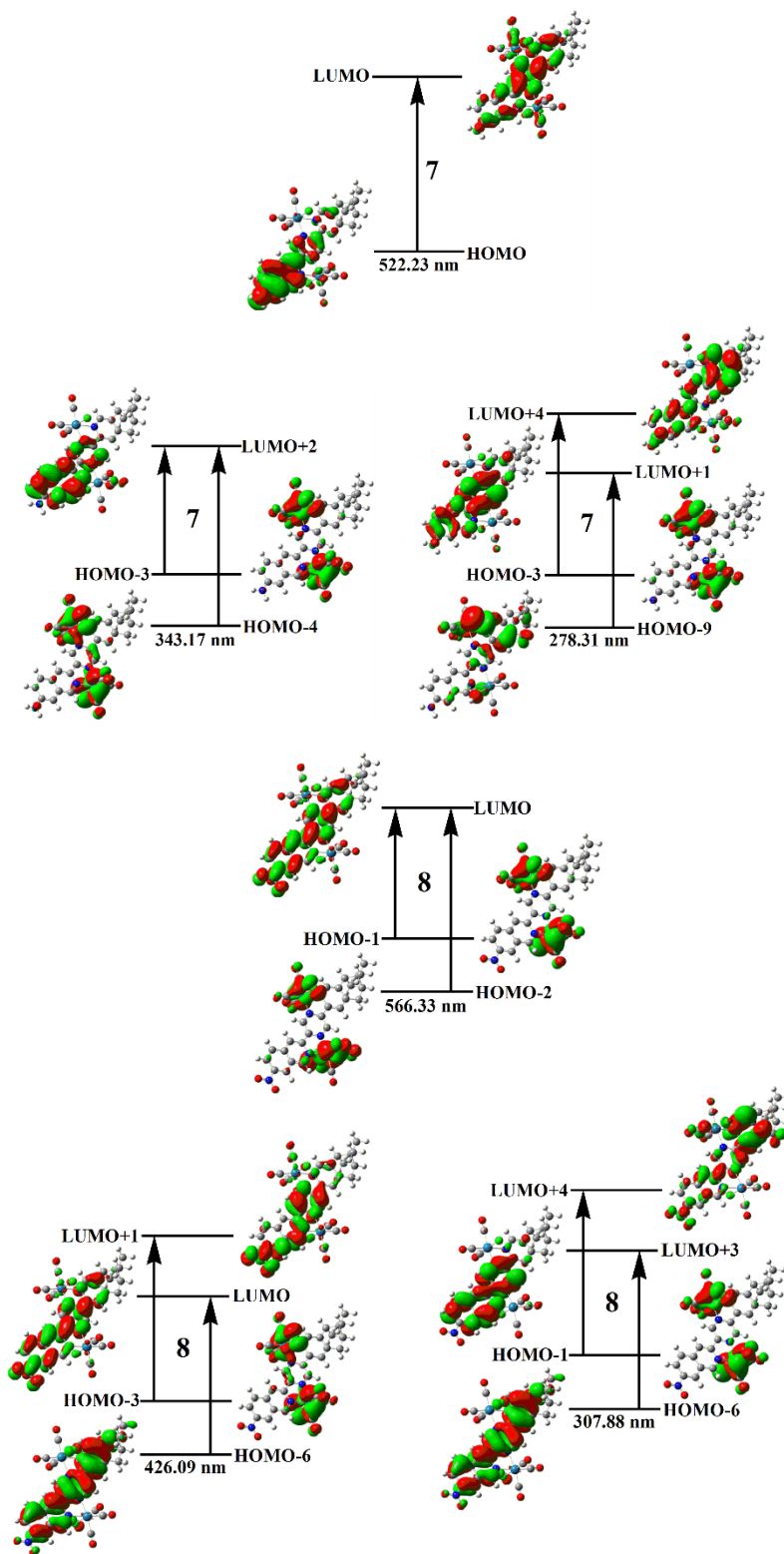| Complex	State	E(eV)	λ_{cal}(nm)	f	Major contribution	Assignments
3	S3	2.35	528.61	0.187	H-2→L (91%)	MLCT/LLCT/ XLCT
	S8	3.08	403.14	0.336	H-7→L (66%)	ILCT
					H→L+1 (18%)	MLCT/LLCT/ XLCT
	S24	3.97	312.07	0.223	H-7→L+1 (77%)	ILCT
4	S3	2.25	550.73	0.164	H-2→L (64%)	MLCT/LLCT/ XLCT
					H-1→L (27%)	MLCT/LLCT/ XLCT
	S13	3.06	404.99	0.232	H-6→L (37%)	ILCT
					H-2→L+3 (24%)	MLCT/LLCT/ XLCT
	S42	4.01	309.14	0.325	H-6→L+3 (63%)	ILCT
5	S3	2.26	549.29	0.165	H-2→L (41%)	MLCT/LLCT/ XLCT
					H-1→L (39%)	MLCT/LLCT/ XLCT
	S18	3.13	395.84	0.138	H-2→L+2 (22%)	MLCT/LLCT/ XLCT
					H-7→L (21%)	ILCT
	S48	4.07	304.96	0.280	H-7→L+3 (78%)	ILCT
6	S3	2.37	523.33	0.156	H-2→L (92%)	MLCT/LLCT/ XLCT
	S7	2.92	424.59	0.649	H-4→L (89%)	ILCT
	S21	3.69	336.24	0.184	H-4→L+1 (60%)	ILCT
					H-10→L (18%)	XLCT
	S33	4.19	296.23	0.210	H-7→L+1 (74%)	ILCT
7	S3	2.37	522.23	0.482	H→L (69%)	ILCT
	S17	3.61	343.17	0.084	H-3→L+2 (63%)	MLCT/LLCT/ XLCT
					H-4→L+2 (21%)	MLCT/LLCT/ XLCT
	S47	4.45	278.31	0.064	H-9→L+1 (37%)	ILCT/ XLCT
					H-3→L+4 (12%)	MLCT/LLCT/ XLCT
8	S3	2.19	566.33	0.113	H-2→L (63%)	MLCT/LLCT/ XLCT
					H-1→L (30%)	MLCT/LLCT/ XLCT
	S10	2.91	426.09	0.506	H-6→L (48%)	ILCT
					H-3→L+1 (41%)	MLCT/LLCT/ XLCT
	S38	4.03	307.88	0.177	H-1→L+4 (34%)	MLCT/LLCT/ XLCT
					H-6→L+3 (22%)	ILCT
9	S4	2.37	523.50	0.158	H-3→L (65%)	MLCT/LLCT/ XLCT
					H-3→L+1 (18%)	MLCT/LLCT/ XLCT
	S35	3.69	336.32	0.206	H-10→L (22%)	ILCT
					H-7→L+1 (21%)	ILCT
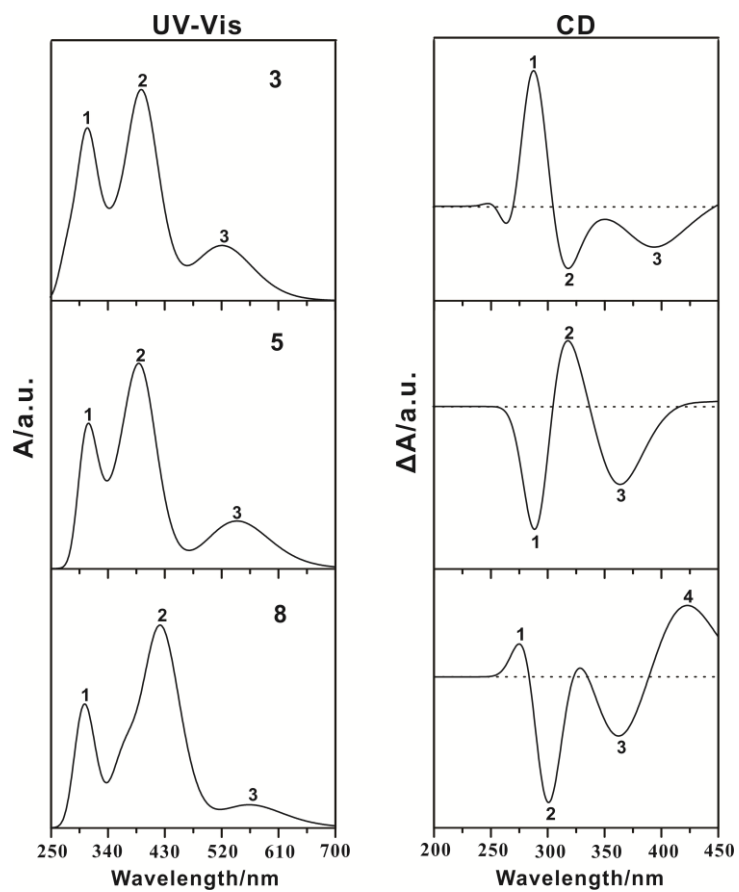
Figure S6. Calculated UV−Vis (left) and CD (right) spectra in the solution phase for complexes **3**, **5** and **8**.

LUMO

3

HOMO-2
528.61 nm
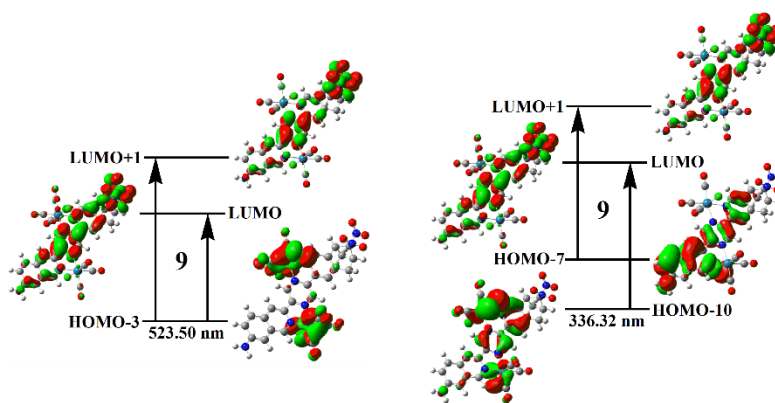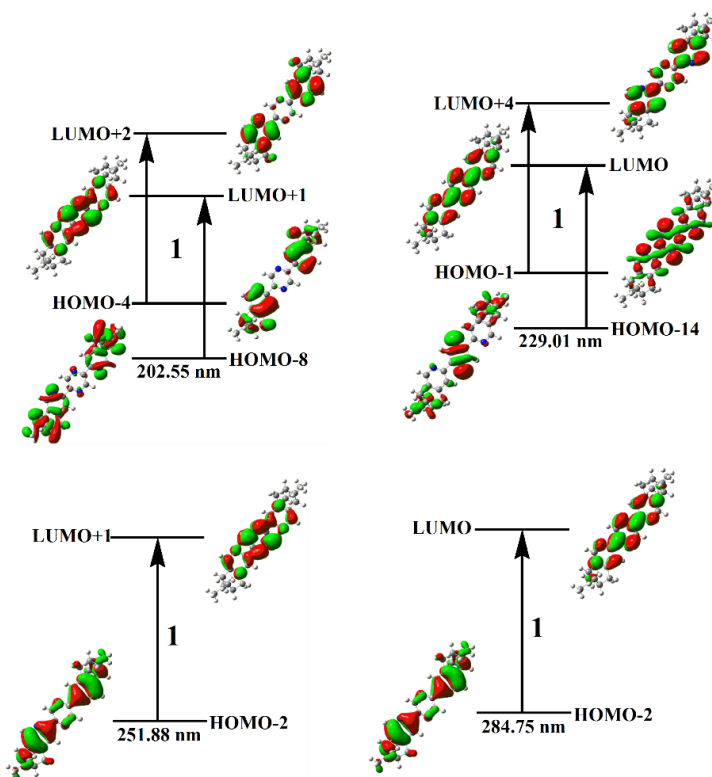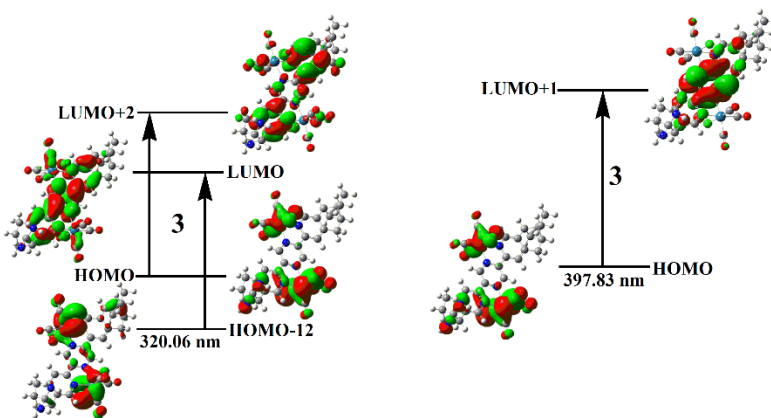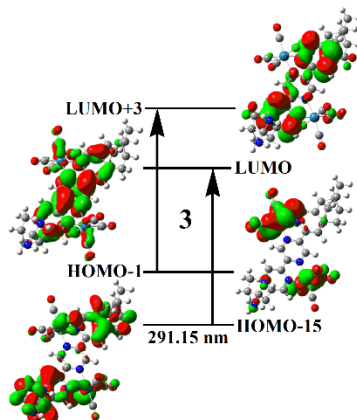
LUMO+1

LUMO

3

HOMO

HOMO-7

403.14 nm

LUMO+1

3

HOMO-7

312.07 nm

LUMO

4

HOMO-1

HOMO-2

550.73 nm

LUMO+3

LUMO

4

HOMO-2

HOMO-6

404.99 nm

LUMO+3

4

HOMO-6

309.14 nm

20

LUMO

5

HOMO-1

HOMO-2

549.29 nm

LUMO+2

5

HOMO-2

LUMO

HOMO-7

395.84 nm

LUMO+3

5

HOMO-7

304.96 nm

LUMO

6

HOMO-2

523.33 nm

LUMO

6

HOMO-4

424.59 nm

LUMO+1

6

LUMO

HOMO-4

HOMO-10

336.24 nm

LUMO+1

6

HOMO-7

296.23 nm

LUMO ──

7

HOMO ──
522.23 nm

LUMO+2

7

HOMO-3 ──
HOMO-4
343.17 nm

LUMO+4

LUMO+1

7

HOMO-3 ──
HOMO-9
278.31 nm

LUMO

8

HOMO-1 ──
HOMO-2
566.33 nm

LUMO+1 ──
LUMO

8

HOMO-3 ──
HOMO-6
426.09 nm
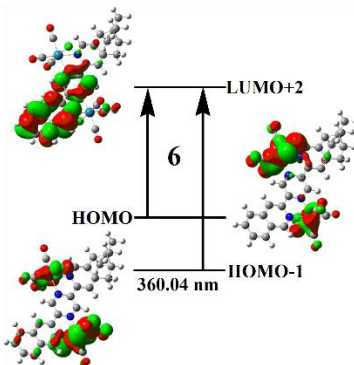
LUMO+4

LUMO+3

8
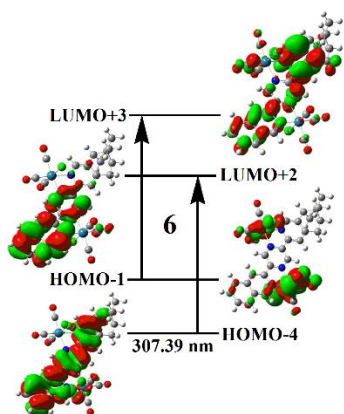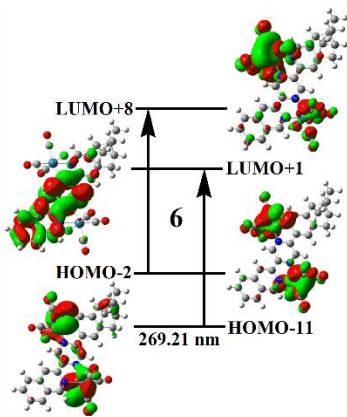
HOMO-1 ──
HOMO-6
307.88 nm

Figure S7. Molecular orbital isosurfaces involved in the main electron transitions of complexes **3-9** at the TDB3LYP/ BSII (BSIII for metal Re) level of theory.
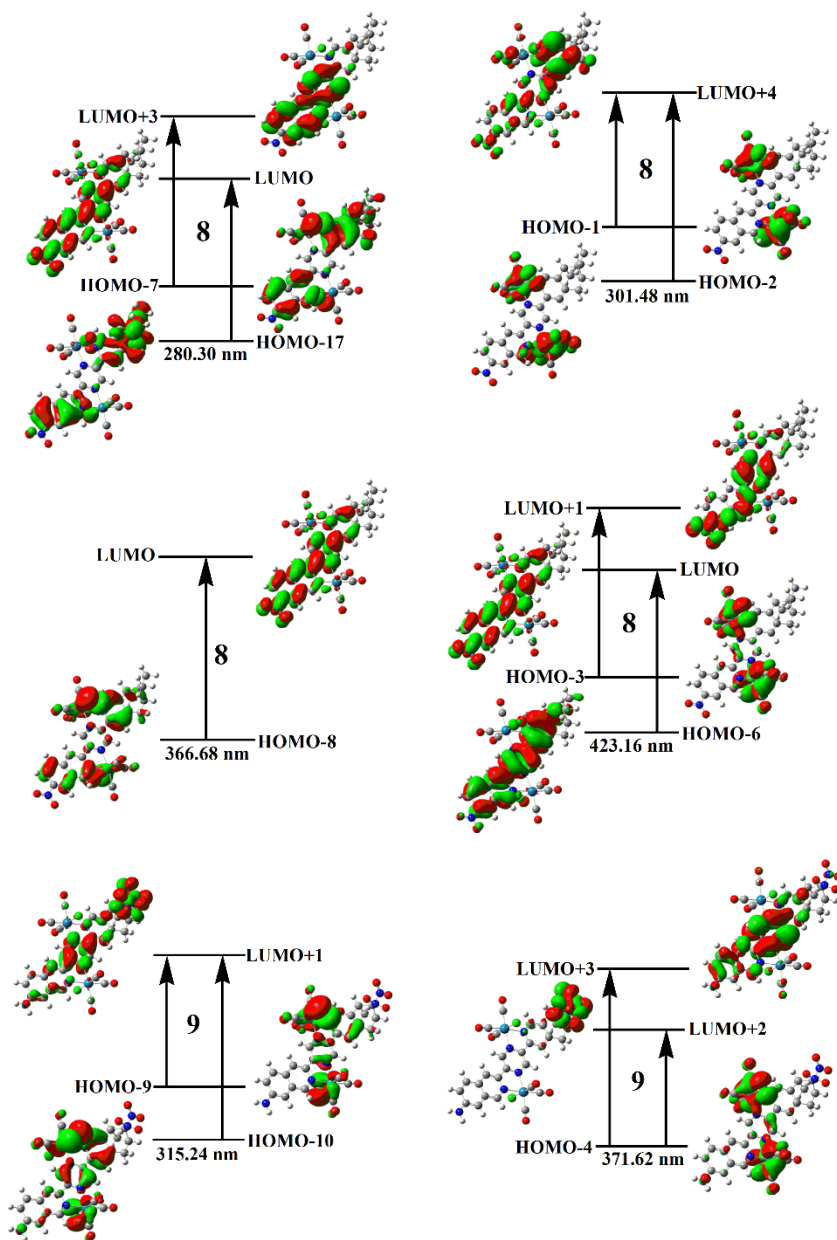
LUMO+8

LUMO+1

HOMO-2

6

269.21 nm

HOMO-11

LUMO+3

LUMO+2

HOMO-1

6

307.39 nm

HOMO-4

LUMO+2

HOMO

6

360.04 nm

HOMO-1

LUMO+4

HOMO-1

7

277.18 nm

HOMO-3

LUMO+2

HOMO-5

7

308.72nm

HOMO-6

LUMO+2

LUMO+1

HOMO

7

368.33 nm

HOMO-4
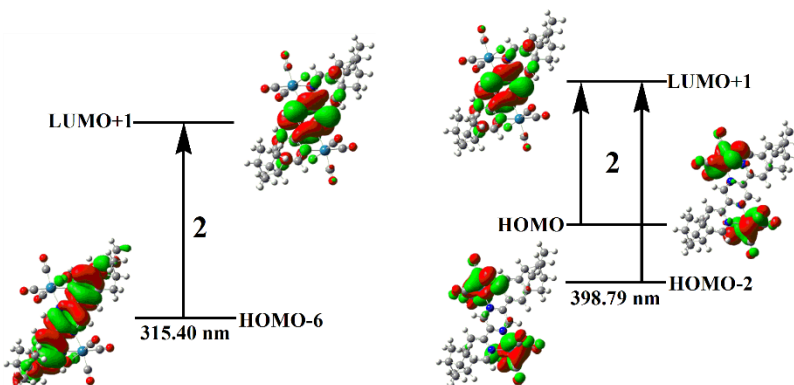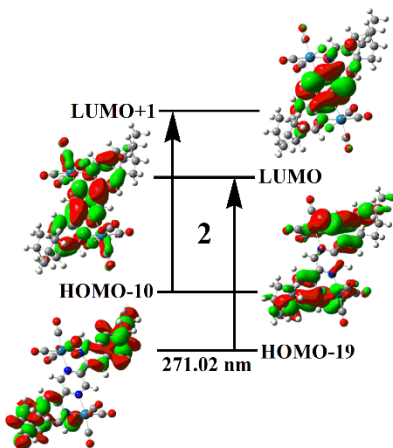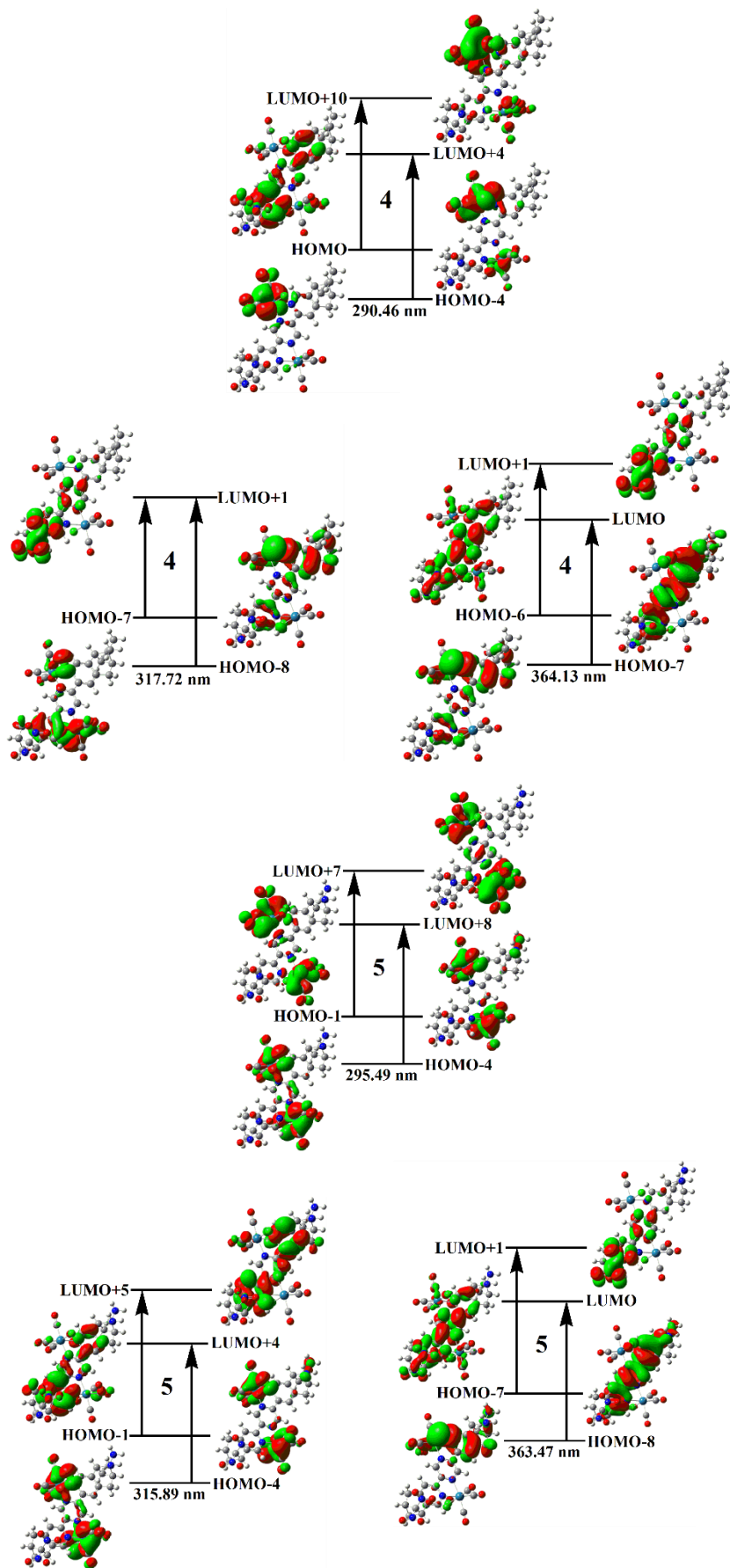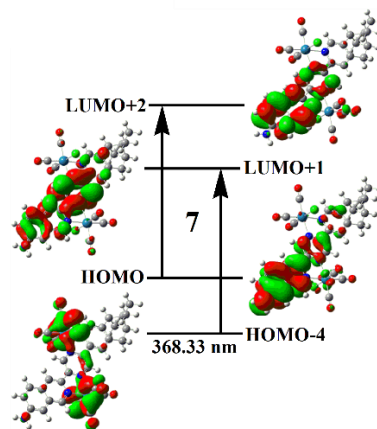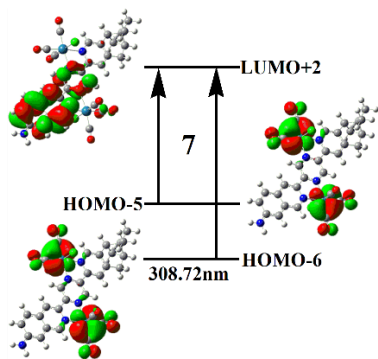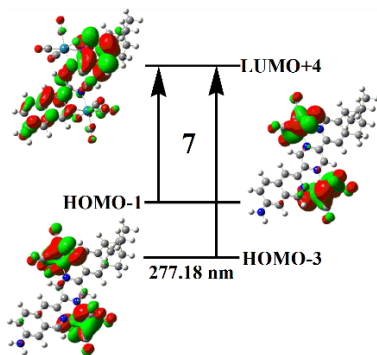
Figure S8. Molecular orbitals involved into the main CD transition of ligand **1**, complexes **2-9**.